

Supplementary Information

A Microfluidic ExoSearch Chip for Multiplexed Exosome Detection Towards Blood-based Ovarian Cancer Diagnosis

Zheng Zhao, Yang Yang, Yong Zeng, Mei He

Reagents, antibodies and human samples.

The detection antibodies used in this study are CA-125 (B2626M, Meridian Life Science) conjugated with Alexfluor-488, EpCAM (323/A3, Thermo Scientific Pierce) conjugated with Alexfluor-550, CD24 (eBioSN3, eBioscience) conjugated with Alexfluor-633, HE4 (EPR4743, abcam) conjugated with Cyanine 5. The capture antibodies used in this study are CD9 biotin (C3-3A2, Ancell), CD81 biotin (1.3.3.22, Ancell), and CD63 biotin (H5C6, BioLegend). Exosome capture beads (Dyna beads M-270 Streptavidin, 2.8 μm in diameter) were obtained from Invitrogen and coupled with capture antibody through biotin-streptavidin linkage per the instruction, generating typical binding capacity of $\sim 10 \mu\text{g}$ biotinylated antibody per 1 mg of beads. Antibody-coated beads (0.1 mg/mL) was introduced into microfluidic device for mixing with human blood plasma at variable flow rates precisely controlled by a programmable syringe pump. The human blood plasma were obtained from University of Kansas Cancer Center's Biospecimen Repository following consents and standard protocols.

Table. The list of human samples used in this study

| OvCa Patients | Age | Cancer stage | Treatment | Sample |
|---------------|------------|---------------|------------------|---------------|
| 1. | 72 | III | N | Blood Plasma |
| 2. | 67 | II | N | Blood Plasma |
| 3. | 70 | III | N | Blood Plasma |
| 4. | 80 | III | N | Blood Plasma |
| 5. | 65 | III | N | Blood Plasma |
| 6. | 61 | III | N | Blood Plasma |
| 7. | 76 | III | N | Blood Plasma |
| 8. | 74 | II | N | Blood Plasma |
| 9. | 64 | III | N | Blood Plasma |
| 10. | 78 | III | N | Blood Plasma |
| 11. | 66 | III | N | Blood Plasma |
| 12. | 75 | II | N | Blood Plasma |
| 13. | 67 | III | N | Blood Plasma |
| 14. | 55 | III | N | Blood Plasma |
| 15. | 53 | III | N | Blood Plasma |
| | Age | Status | Treatment | Sample |

| | | | | |
|----|----|---------|---|--------------|
| 1. | 51 | Healthy | - | Blood Plasma |
| 2. | 53 | Healthy | - | Blood Plasma |
| 3. | 50 | Healthy | - | Blood Plasma |
| 4. | 52 | Healthy | - | Blood Plasma |
| 5. | 53 | Healthy | - | Blood Plasma |

De-identified samples and matching information were obtained from University of Kansas Cancer Center's Biospecimen Repository following consents and standart protocols.

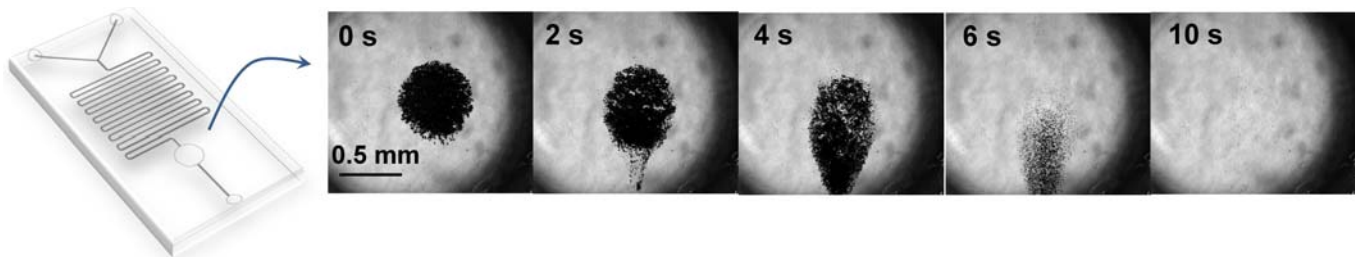


Figure s1. The sequential snapshots showing the release process of bead aggregates after switching off the magnetic field during continuous flow in ExoSearch chip.

Characterization of non-specific adsorption and cross-reactivity for on-chip immunomagnetic assay

In order to characterize the non-specific adsorption and cross-reactivity of antibodies used in this study, the negative and positive control experiments were designed and conducted in parallel. The fluorescence background of magnetic beads themselves was measured, compared with fluorescence intensity after detection antibody probing and washing, without introducing plasma exosome samples. The slight auto-fluorescence of capture beads and negligible non-specific adsorption fluorescence were observed. There is no cross-reaction between antibodies we used in this study. The positive control (ovarian cancer patient plasma exosomes) showed strong fluorescence signals after antibodies probing (CA-125, EpCAM, and CD24). However, we did not observe acceptable positive response from HE4 antibody probing. In order to achieve the accurate fluorescence readout, we set the same image threshold (0-255 grey scale). Meanwhile, for each sample analysis, we collected one image of PDMS microchamber as the background, one image of beads aggregate right before antibody probing step, and one image of beads aggregate after antibody probing and washing step. The difference of fluorescence signals before and after antibody probing was calculated, and then normalized to background. We designed a macro function of ImageJ for randomly picking up 1000 points in the consistent area of sample signals and measuring the average of mean gray value of fluorescence intensity.

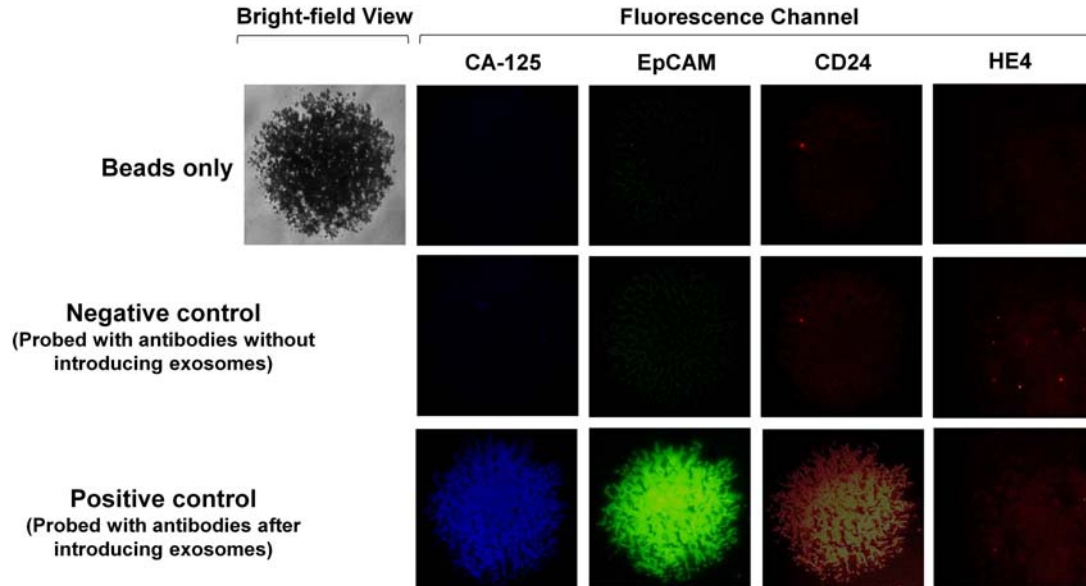


Figure s2. CCD captured microscopic images of bead aggregates under negative and positive control experimental conditions. Image size is 200 $\mu\text{m} \times 200 \mu\text{m}$.

Western blotting

Tris-glycine pH 8.3, 4-12% precast polyacrylamide slab mini-gels with Blot Module (BioRad) was used for performing Western blottings, following standard protocol. Ultracentrifugation-purified exosomes were lysed and prepared by adding protease inhibitors and running buffer (0.1% SDS), and heating at 65°C for 5 min. After electrophoresis at 125 V for 2 h, gels were electrotransferred to cellulose membranes (0.2 μm) at 25 V for 2.5 h in ice bucket. After twice washing (1 \times PBS, 0.5% Tween 20, pH 7.4), the membranes were blocked with 5% dry milk overnight at 4°C with shaking. The solution of primary biotinylated antibody (1:1500) was added into blocking buffer for 2-h incubation with shaking at room temperature. After incubation, the membrane was washed 3 times for 10 min each. The secondary antibody streptavidin-HRP (Invitrogen, ELISA grade, 1.2 mg/mL) diluted 1:2500 in the blocking solution was added for 1-h incubation at room temperature with agitation. After that, the washing step was repeated three times. The membrane was subsequently developed with chromogenic substrate reagent (BioRad) until the desired band intensity was achieved. Imaging was performed by using ChemiDoc imager (BioRad).

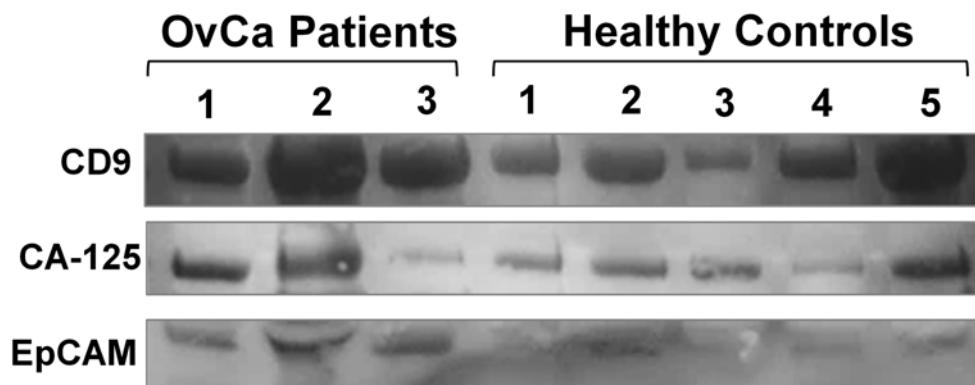


Figure s3. Western blotting analysis of expression levels of exosomal surface marker CD9, CA-125, and EpCAM. The plasma exosome samples were prepared from ovarian cancer patients and healthy controls using standard ultracentrifugation.

Sample Size Justification

Estimating the required sample size to adequately train developed diagnostic assay is of great practical importance¹. We calculated the required sample size for evaluating diagnostic accuracy, by comparing the area under a ROC curve with a null hypothesis value of 0.5. The sample size takes into account the required significance level of 0.05 and 80% power of the test. The statistical power 0.8 and sample ratio of 3 were chosen for statistical judgment with 0.2 probability of type I error α and 0.2 probability of type II error. Thus the sample size computational table was listed below in Table s1. The sample size of total 20 (15 ovarian cancer patients and 5 healthy controls) is adequate to evaluate diagnostic accuracy with acceptable diagnostic power.

Table s1: Sample size justification with desired errors

| | | Type I error- α | |
|------------------------|------|------------------------|-------|
| | | 0.20 | 0.05 |
| Type II error- β | 0.20 | 15+5 | 27+9 |
| | 0.05 | 27+9 | 42+14 |

Diagnostic Accuracy^{2,3}

Sensitivity and specificity are terms used to evaluate a clinical test. Receiver operator characteristic curve is a plot of (1-specificity) of a test on the x-axis against its sensitivity on the y-axis for all possible cut-off points. The area under this curve (a. u. c.) represents the overall accuracy of a test, with a value approaching 1.0 indicating a high sensitivity and specificity. The a.u.c. is a global measure of diagnostic accuracy. By comparison of areas under ROC curves, we can estimate which one of the tests is more suitable for distinguishing health from disease. The accuracy classification for a diagnostic test is listed below.

Table s2. Accuracy classification by a.u.c. for a diagnostic test

| a.u.c. Range | Classification |
|--------------------|----------------|
| 0.9 < a.u.c. < 1.0 | Excellent |
| 0.8 < a.u.c. < 0.9 | Good |
| 0.7 < a.u.c. < 0.8 | Worthless |
| 0.6 < a.u.c. < 0.7 | Not good |

We statistically analyzed the specificity and sensitivity using receiver operator characteristic curves for on-chip measurements (expression levels of CA=125, EpCAM, and CD24), compared to conventional benchtop measurements (Bradford assay of total exosome protein, and NTA of exosome particle concentration), from 20 human subjects ($n_{OvCa}=15$, $n_{healthy}=5$). On-chip assay of multiple exosomal proteins showed excellent diagnostic accuracy (CA-125 a.u.c.=1.0; EpCAM a.u.c.=1.0; CD24 a.u.c.=0.91), which was comparable with conventional Bradford assay of total exosome proteins (a.u.c.=1.0). However, NTA assay of exosome concentration was unable to give acceptable accuracy using particles number as the diagnostic value (a.u.c.=0.67).

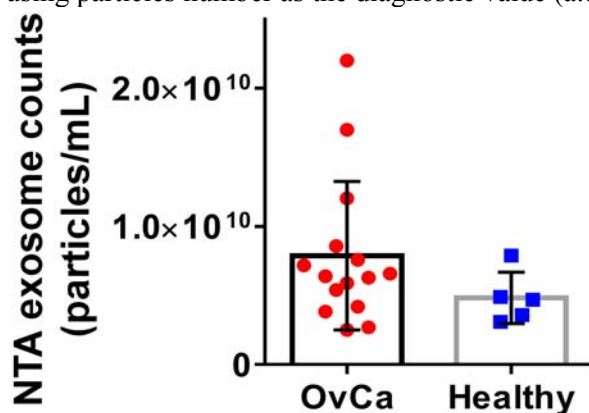


Figure s4. The plasma exosome particle concentrations from 20 human subjects measured by NTA ($n_{\text{OvCa}}=15$, $n_{\text{healthy}}=5$). Slightly higher average amount of plasma exosomes (1.5 fold) was observed from ovarian cancer patients, compared to healthy controls ($p=0.25$). The difference was not significant.

Table s3. Diagnostic accuracy analysis using the receiver operating characteristic curve

| Test Variables | ExoSearch chip | | | Bradford Assay/ Total Exosomal Protein | NTA/ Particle Concentration |
|--------------------------------|----------------|----------------|----------------|--|--------------------------------|
| | CA125 | EpCAM | CD24 | | |
| ROC Curve Area | 1.000 | 1.000 | 0.9067 | 1.000 | 0.6750 |
| Standard Error | 0.000 | 0.000 | 0.0903 | 0.000 | 0.1332 |
| 95% Confidence Interval | 1.000 To 1.000 | 1.000 To 1.000 | 0.729 To 1.084 | 1.000 To 1.000 | 0.413 To 0.936 |
| P Value | 0.0010 | 0.0010 | 0.0078 | 0.0009 | 0.2477 |

References:

1. Suresh, K. & Chandrashekara, S. Sample size estimation and power analysis for clinical research studies. *Journal of human reproductive sciences* **5**, 7-13 (2012).
2. van Stralen, K.J. *et al.* Diagnostic methods I: sensitivity, specificity, and other measures of accuracy. *Kidney international* **75**, 1257-1263 (2009).
3. Zou, K.H., O'Malley, A.J. & Mauri, L. Receiver-operating characteristic analysis for evaluating diagnostic tests and predictive models. *Circulation* **115**, 654-657 (2007).